

MODELING WATER QUALITY USING TERRA/MODIS 500M SATELLITE IMAGES

M. S. Wong ^{a,*}, J. E. Nichol ^a, K. H. Lee ^b, N. Emerson ^a

^a Department of Land Surveying and Geo-Informatics, The Hong Kong Polytechnic University, Hung Hom, Kowloon, Hong Kong - (m.wong06@fulbrightweb.org)

^b Earth System Science Interdisciplinary Center (ESSIC), University of Maryland (UMD), College Park, USA

KEY WORDS: Chlorophyll a, Coast, MODIS, Suspended Solids, Turbidity, Water quality

ABSTRACT:

A study was conducted in Hong Kong with the aim of deriving algorithms for the retrieval of turbidity, chlorophyll a and suspended solids concentrations from Terra/MODIS 500m level 1B reflectance data. Rigorous atmospheric correction using Radiative Transfer Model coupled with the inputs of AERONET data and MODIS atmospheric products was carried out for deriving the water leaving reflectances. The in-situ measurements were compared with coincident water leaving reflectances using different sets of empirical algorithms. Due to the high variation of water quality in Hong Kong, the in-situ data were divided into three groups based on the spatial locations of the measurements: east zone (similar to case I water), west zone (similar to case II water) and harbour zone (in between case I and case II water). Significant correlations were observed between water-leaving reflectances and in-situ marine data on the three zones while only moderate correlations can be found on those with the entire dataset. These suggest the single empirical algorithm may not be applicable on the areas with high variation of water quality and MODIS 500m data are feasible for water quality retrieval in a local scale.

1. INTRODUCTION

Hong Kong, an affluent city with a service-based economy is situated at the mouth of the Pearl River, whose delta region, spanning Hong Kong, Macau and Guangdong Province of China, has undergone lightning-paced industrial and urban development over the last 20 years. Accompanying this, the Pearl River Delta (PRD) region itself has suffered many adverse environmental changes including sea level rise, increased storminess and changes in salinity, sea surface temperature, nutrient, phytoplankton and sediment content, and sediment transport profiles. The economy and activities of the coastal cities of the PRD are directly affected by such changes. Increased salinity in the domestic water supply, with adverse effects for residents and tourists alike, has recently gained wide publicity.

Traditionally, water quality monitoring in Hong Kong relies on fixed stations by collecting water samples and analyzing in the laboratory. The problems of point sampling at fixed stations may be overcome by the use of satellite images which potentially offer wide area coverage, as well as long-term and continuous marine measurements. Until recently, no suitable marine satellite sensors were available, since the most commonly used earth monitoring satellites LANDSAT and SPOT were calibrated for land. Thus their signal to noise ratio for low reflectance water surfaces was inadequate to obtain meaningful data. Furthermore, in a sub-tropical region such as Hong Kong, the low repeat cycles and high cost of these satellites limited their usefulness for monitoring constantly changing phenomena such as water quality.

These problems can be solved until the modern satellite sensors have been launched eg. SeaWiFS, Terra/MODIS, Aqua/MODIS and MERIS. These sensors provide the feasibility for monitoring water quality and biological elements (Hu et al.,

2004; Miller and Mckee, 2004; Dall'Olmo et al., 2005; Chen et al., 2007; Wong et al., 2007). The MODIS sensors on NASA's Terra and Aqua spacecrafts were launched in 1999 and 2002 respectively. They are multi-spectral sensors with several wavebands designed for the sensing of earth's environment including atmosphere, land, and ocean.

The ways of modeling water quality can be divided into empirical and analytical methods. The empirical methods correlate the in-situ measurements with satellite reflectances in certain wavelengths. This method is applicable in local and regional scales, but not universal. The limitation of empirical method is the requirement of sufficient in-situ data which are not always able to obtain in some remote areas. The analytical method studies the bio-optical model which based on the absorption and scattering of underwater elements and its relationship with spectral wavelengths. The complicated algorithms normally induce certain errors during the rigorous modeling.

2. DATA USED AND STUDY AREA

Hong Kong waters, can be divided into three zones based on influences from different geographical sources (Morton and Wu, 1975; Wu, 1988). The western waters (Deep Bay) which are affected by Pearl River estuarine region are turbid. The eastern waters (Mirs Bay) are influenced by the Pacific currents, while the central waters are influenced by both Pearl River, Pacific currents, as well as by local residential and industrial effluents into the Victoria Harbour (Yeung, 1998). During 2001 to 2005, the average turbidity of Hong Kong is quite high at around 12 ntu. The average chlorophyll a and suspended solid concentrations are about 6 mg/l and 3 mg/l respectively.

* Corresponding author: Man Sing Wong, email: m.wong06@fulbrightweb.org; wongmansing.charles@gmail.com

Marine monitoring system in Hong Kong, still relies on the Conductivity-Temperature-Depth (CTD) profilers developed in 1986 (EPD, 2004) for water quality monitoring. They are deployed at fixed points and data is collected biweekly and monthly. Figure 1 shows the locations of these monitoring stations. Three levels in the water column are measured: (i) surface (1m below sea surface), (ii) middle (half of the sea depth) and (iii) bottom (1m above seafloor). In this study, the in-situ surface (1m below sea surface) data are only utilized because they have stronger correlations with image surface reflectances. In addition, twelve cloud-free Terra/MODIS images were acquired for modeling of turbidity, chlorophyll II a and suspended solids on year 2001, 2002 and 2005.

km data because their finer resolutions show more spatial variation over the small study area. Terra/MODIS images, rather than Aqua/MODIS, were selected since Terra spacecraft crosses Hong Kong at 10:30am local time. This time is close to the EPD's data collection time (11 to 12 noon), allowing the data to easily satisfy the definition of in-situ (Woodruff et al., 1999). Acquiring in-situ data corresponding to the satellite images is difficult especially for ocean and water studies. Miller and Mckee (2004) made use of 52 in-situ measurements during six field campaigns, for mapping suspended matter with Terra/MODIS 250m resolution images. Chen et al. (2004) classified water quality in the Pearl River estuary and its adjacent coastal waters of Hong Kong using clustering method based on 58 in situ water quality dataset and 30 samples from SeaWiFS and AVHRR images.

This study aims to demonstrate the usefulness of MODIS spectral images for water quality measurements using in-situ water quality monitoring data (turbidity, chlorophyll II a, suspended solids) provided by the Hong Kong Environmental Protection Department (EPD). A total of three zones were decided for Case I water (east zone), Case II water (west zone) and in-between Case I and Case II water (Victoria harbour) (Figure 1). Detailed water quality study was carried out by evaluating the empirical algorithms for each case. A total of 59 in-situ water samples were collected on year 2001, 2002 and 2005. This study reveals the ability of modeling water quality using in-situ data on different days of years while previous studies rely on the measurements from field campaigns taking on only one or two days.

3. ATMOSPHERIC CORRECTION

Atmospheric aerosols are always shown in the satellite images especially in the south-east region of China. The MODIS satellite images affected by spatially and temporary aerosols should be corrected while these may induce certain errors on water quality retrieval. In this study, the aerosols were corrected by Radiative Transfer Model (RTM) coupled with the inputs of MODIS aerosol products (MOD04 C005) and AERONET inversion data (refractive index and size distribution). Figure 2 shows schematic diagram of the atmospheric correction for MODIS L1B images. The microphysical/optical properties such as aerosol inversion data (refractive index and size distribution) were acquired from the Hong Kong AERONET station. Since the Hong Kong AERONET was established from year 2005 and there are no aerosol direct measurements beforehand, the inversion data from year 2005 to 2007 were adopted by re-grouping into four seasons. The average seasonal aerosol inversion data were inputted as the microphysical properties in RTM. Meanwhile, the MODIS aerosol products MOD04 (collection 5) were acquired from NASA Goddard Earth Science Distributed Active Archive Center (DAAC). The MOD04 data were then resampled to 500m resolution and inputted in the RTM. Such AOT and microphysical data were inputted into the Second Simulation of a Satellite Signal in the Solar Spectrum (6S) (Vermote et al., 1997) RTM for deriving the atmospheric corrected surface reflectances.

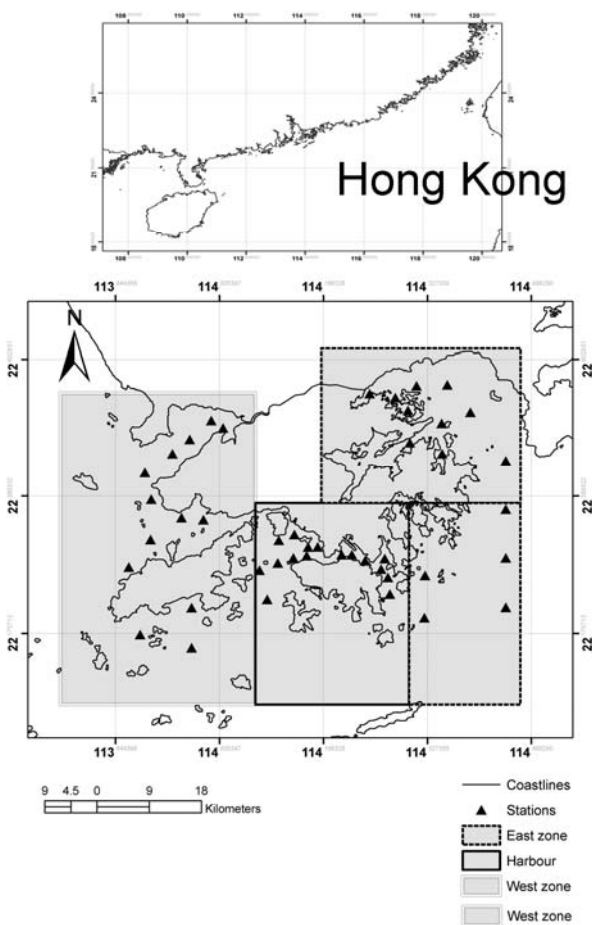


Figure 1. Map of Hong Kong study areas and sampling stations

Terra/MODIS sensor provides high radiometric sensitivity (12 bit) data in 36 spectral bands ranging in wavelength from 405nm to 14.4µm. Two bands are imaged at a nominal resolution of 250m at nadir, five bands at 500m, and the remaining 29 bands at 1km. All the bands were selected particularly to minimize the impact of absorption by atmospheric gases (Justice et al., 2002). Because of its advantages, MODIS images are being used increasingly to detect the change of water environment. Twelve sets of Terra/MODIS level 1B images were acquired through the NASA Goddard Earth Science Distributed Active Archive Center (DAAC). They were compared with 44 stations available from the EPD's monitoring system (Figure 1). MODIS 500m images were selected for modeling instead of 1

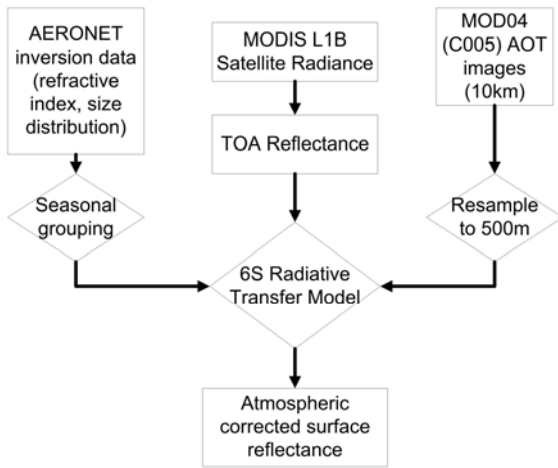


Figure 2. Flowchart of atmospheric correction

4. METHODOLOGY

The Hong Kong water quality is complicated to retrieve with only one or universal empirical algorithm since several water cases shown in Hong Kong. Thus, this study divides the Hong Kong water into three zones: east zone (similar to case I water), west zone (case II water) and Victoria harbour region. Three different sets of empirical algorithms were then derived based on in-situ measurements. In the study, empirical regression algorithms were adopted from previous studies (Eq 1). In order to examine the accuracy of each model, the correlation coefficient, Root Mean Square Errors (RMSE) (Eq 2) and P value (the level of significance) were evaluated (Milton and Arnold, 1995) for each model.

$$\text{Marine data} = A_0 + \sum_{i=1}^k A_i (\text{MODIS}_i) \tag{1}$$

$$\text{RMSE} = \sqrt{\frac{1}{N-2} \sum_{i=1}^N (x_{\text{in-situ}} - x_{\text{MODIS}})^2} \tag{2}$$

where $x_{\text{in-situ}}$ is in-situ data, x_{MODIS} is modeled data estimated from satellite.

4.1 Turbidity

Turbidity is a general measurement of water clarity and reflects the degree of cloudiness by sediment. The growth of phytoplankton (chlorophyll a) and suspended solids makes the water turbid and the values are always high near the coasts and estuaries. A number of researches have been demonstrated the estimation of turbidity using different satellite sensors, such as AVHRR (Woodruff et al., 1999; Aguirre-Gomez, 2000) and Landsat TM (Tassan, 1987). Koponen et al. (2001) noted the turbidity is proportioning to the square of MODIS channel 1 reflectances in a study of lake (Eq 3). Chen et al. (2007) suggested similar algorithm which has strong correlation with in situ data (Eq 4) in Tampa bay. Regression models based on Eq 3 and Eq 4 in three water zones and the entire area were evaluated. The correlation coefficient, P value, RMSE are listed in Table 1.

$$\sqrt{T} \propto L_{\text{MODIS-C1}} \tag{3}$$

$$T = 1203.9 \cdot L_{\text{MODIS-C1}}^{1.087} \tag{4}$$

Method	R	RMSE	P	N	Data range (ntu)
Harbour					
T1 Eq 3	0.68	1.31	0.004	15	5.4-12.1
T2 Eq 4	0.67	1.32	0.005	15	5.4-12.1
East zone					
T3 Eq 3	0.67	0.58	0.001	23	4.6-7.5
T4 Eq 4	0.67	0.58	0.001	23	4.6-7.5
West zone					
T5 Eq 3	0.68	1.46	0.001	21	11.7-19.2
T6 Eq 4	0.68	1.46	0.001	21	11.7-19.2
Entire HK					
T7 Eq 3	0.60	3.33	0.001	59	4.6-19.2
T8 Eq 4	0.60	3.33	0.001	59	4.6-19.2

Table 1. Accuracy assessment of turbidity models

As mentioned in previous section, the water turbidity in west zone is especially high due to the sewage and discharges from Pearl river, the range of turbidity values is from 11.7 to 19.2 ntu. In contrast with west zone, the east zone has lower range of turbidity values (4.6 to 7.5 ntu) which is similar to case I water. In Victoria Harbour zone, the values are in between east and west zones where the local sewage and discharges influence the water quality.

The Table 1 noticed that the fairly correlations were achieved from models on three different zones and the entire Hong Kong territories. The correlation coefficients from Eq 3 and Eq 4 have similar correlation coefficient (R~0.68). For the entire area, R=0.61 and RMSE~3.34 were observed. It is also noticed that the evaluating tools such as RMSE, P values and confidence intervals have similar findings from Eq 3 and Eq 4. The results are then suggested either Eq 3 and Eq 4 is applicable and feasible on modeling the water turbidity on three different water scenarios. Figure 3 demonstrates an example of turbidity map based on the models T1, T3, T6 on Nov 29, 2005.

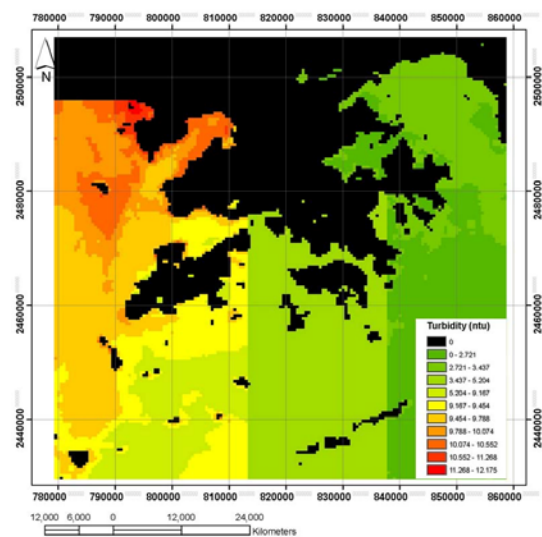


Figure 3. Turbidity map (derived from Eqs T1, T3, T6 on Nov 29, 2005)

4.2 Chlorophyll a (Chl a)

Phytoplankton (chlorophyll a) is one of the key substances under water and it is the base-level substance in the aquatic food-chain. Chl a has been researched for using the in-situ data and satellite observation for couple of years. NASA/GSFC Ocean Color group developed the OC3M empirical chlorophyll algorithms for global chlorophyll monitoring. Gons (1999) demonstrated using band ratio (R704/R672) to retrieval Chl a concentration. Dall’Olmo et al. (2005) used R725/R675, Dekker (1993) and Gitelson et al. (1993) used the ratio of R680/R710 to retrieve the Chl a concentration. While due to the limited spectral coverage of MODIS 500m image, there is a lack of channel between 700 to 800nm which has high reflectance values (lower absorption) of Chl a concentration (Kneubühler et al., 2005). While Mobley (1994) noted that the Chl a has two absorption peaks at 430nm and 665nm, in respect, the MODIS channel 3 and channel 1 (459-479 nm and 620-670nm) are fitted for this purpose. Han and Jordan (2005) show the combination of band ratio methods using Landsat ETM image for modeling the Chl a concentration in Florida. They tested a set of models with logarithmically transformed Chl data, and logarithmically transformed reflectances. The strongest correlation was observed using the Eq 5 and Eq 6 which are evaluated in the study.

$$\log(\text{Chl a})=A_0+A_1 \cdot \log\left(\frac{\text{MODIS}_i}{\text{MODIS}_k}\right) \quad (5)$$

$$\log(\text{Chl a})=A_0+A_1 \cdot \left(\frac{\log(\text{MODIS}_i)}{\log(\text{MODIS}_k)}\right) \quad (6)$$

Method	R	RMSE	P	N	Data range (ntu)
Harbour					
C1 Eq 5	0.66	0.25	0.006	15	0.2-3.3
C2 Eq 6	0.87	0.16	0.001	15	0.2-3.3
East zone					
C3 Eq 5	0.58	0.13	0.003	23	0.7-4.4
C4 Eq 6	0.69	0.10	0.001	23	0.7-4.4
West zone					
C5 Eq 5	0.64	0.07	0.001	21	1.2-3.1
C6 Eq 6	0.86	0.06	0.001	21	1.2-3.1
Entire HK					
C7 Eq 5	0.59	0.17	0.001	59	0.2-4.4
C8 Eq 6	0.63	0.20	0.001	59	0.2-4.4

Table 2. Accuracy assessment of chlorophyll a models

Strong correlations have been observed using Eq 6 with MODIS channel 3 and 1 on west zone and Victoria harbour regions (R=0.875 and R=0.863). The ranges of Chl a concentration on harbour and east zones were relatively small (0.2-3.3 and 1.2-3.1 mg/l) compared to the west zone (0.7-4.4 mg/l). The variability of Chl a in west zone where it is situated on the estuary of Pearl river was recorded with higher concentration of Chl a. Because of the variability of the Chl a concentration caused by the mixture of fresh and sea water, the accuracy of model (C4) from that region is relatively low (R=0.694). From Table 2, it is indicated that Eq 6 works with

stronger correlation and small standard error than Eq 5. The methodology of Eq 6 is based on two high Chl a absorption channels (channel 1 and channel 3) while the increased of Chl a decreases the reflectances on those channels. The fairly correlation was observed for the entire areas (R=0.631 and RMSE = 0.203mg/l for Eq 6). Figure 4 illustrates an example of Chl a map based on the models C2, C4, C6 on Nov 29, 2005.

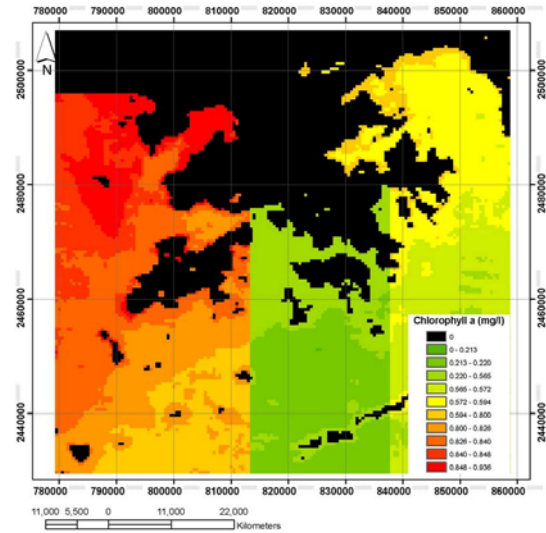


Figure 4. Chlorophyll a map (derived from Eqs C2, C4, C6 on Nov 29, 2005)

4.3 Suspended solids (SS)

There have been a number of researches to map suspended sediments using the visible red channels. It is because the penetration power in visible red region is always sensitive to suspended matter, and it should be the appropriate band region for mapping sediment (Mobley, 1994). Han et al. (2006) developed a suspended sediment index with the Eq 7 for retrieving the suspended sediment from water-leaving radiance. It was proven with strong correlation (R=0.957, N=21) using CMODIS satellite image in the study of Yangtze River estuary (Han et al., 2006). Red channel and green channel were adopted for the inputs of Eq 7. Red channel with spectra (620-670nm) always show its feasibility for modeling SS. The small SS concentration can be detected by green channel with shorter wavelength (545-565nm). Thus the term (MODIS4+MODIS1) works with different spectral reflections for large and small SS concentration. The term (MODIS4/MODIS1) reduces the Chl a interference to the low SS concentration (Li et al., 2002 and Han et al., 2006). In this study, a modified equation (Eq 8) was developed. The rationale is similar to Eq 7 but the term of (MODIS4/MODIS1) is replaced by (MODIS3/MODIS1) which was found more effective to reduce the interference of Chl a (the results from section 4.2). Moreover, a single band regression with red channel was also tested with in-situ data on three decided zones and the entire territories (Eq 9).

$$\log(\text{SS})=A_0+A_1 \frac{\text{MODIS}_i+\text{MODIS}_k}{\text{MODIS}_i/\text{MODIS}_k} \quad (7)$$

$$\log(SS)=A_0+A_1 \frac{\text{MODIS}_i+\text{MODIS}_k}{\log(\text{MODIS}_j)/\log(\text{MODIS}_k)} \tag{8}$$

$$SS=A_1 \cdot \text{MODIS}_i \tag{9}$$

Method	R	RMSE	P	N	Data range (ntu)
Harbour					
S1 Eq 9	0.82	0.84	0.001	15	2.8-8.2
S2 Eq 8	0.89	0.06	0.001	15	2.8-8.2
East zone					
S3 Eq 9	0.54	0.82	0.007	23	1.2-4.8
S4 Eq 8	0.84	0.08	0.001	23	1.2-4.8
West zone					
S5 Eq 9	0.41	4.11	0.06	21	2.9-19
S6 Eq 8	0.86	0.11	0.001	21	2.9-19
Entire HK					
S7 Eq 9	0.62	2.88	0.001	59	1.2-19
S8 Eq 8	0.66	0.20	0.001	59	1.2-19

Table 3. Accuracy assessment of suspended solids models

The moderate correlations (R=0.896, R=0.844 and R=0.861) were obtained from Eq 8 in Victoria harbour region, east and west zone respectively. The RMSEs of those models are 0.060, 0.088 and 0.119 mg/l respectively. It is noticed that the modified equation (Eq 8) performs significantly superior than single red band regression (Eq 9) since it takes the advantage of reducing the interference of chlorophyll where only suspended solids are dominant. Suggested algorithm (Eq 8) also has a stronger correlation than original algorithm (Eq 7) which has a poor correlation R=0.237 and RMSE=0.229mg/l in west zone. Figure 5 shows an example of SS map based on the models S2, S4, S6 on Nov 29, 2005.

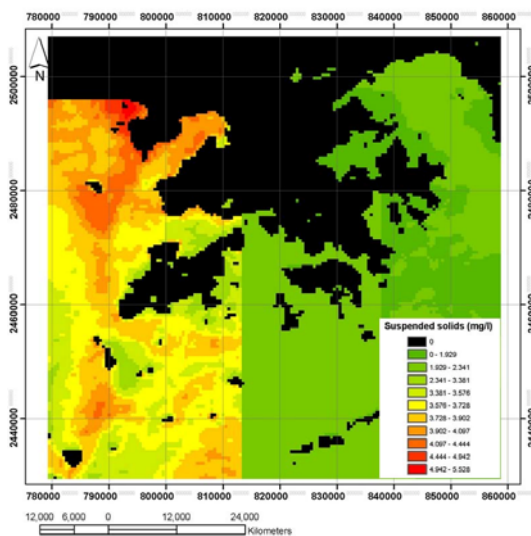


Figure 5. Suspended solids map (derived from Eqs S2, S4, S6 on Nov 29, 2005)

5. DISCUSSION AND CONCLUSION

This study attempts to model turbidity, chlorophyll a and suspended solids concentrations using remote sensing images and in-situ data. Rigorous atmospheric correction was processed on the half kilometre MODIS images for achieving the water-leaving reflectance. Empirical algorithms were developed on three decided zones respectively. The results reveal stronger correlations were achieved with in-situ data than applying algorithm on the entire dataset. Significant correlations were observed between water-leaving reflectances and in-situ marine data using different algorithms adopted and modified based on previous empirical studies. The validation results also showed good correlation between satellite and in-situ measurement data based on three validation methods: correlation coefficient, root-mean-square errors and level of significance. It demonstrates the potential of remote sensing for water quality modeling with 500m resolution in a local scale. This is especially important in Hong Kong water where the water quality has high variation from east to west. Additionally, it is the first ever to map the water quality parameters over Hong Kong based on high resolution MODIS images with a stated accuracy level. This may help in shaping policy decisions at the Hong Kong Environmental Protection Department and Guangdong province for monitoring the coastal waters. The daily water quality maps will be uploaded to the web in the near future.

REFERENCES

Aguirre-Gomez, R., 2000. Detection of total suspended sediments in the North Sea using AVHRR and ship data. *International Journal of Remote Sensing*, 21, pp. 1583-1596.

Chen, Z.Q., Hu, C.M., Muller-Karger, F., 2007. Monitoring turbidity in Tampa Bay using MODIS/Aqua 250-m imagery. *Remote Sensing of environment*, 109(2), pp. 207-220.

Dall'Olmo, G., Gitelson, A.A., Rundquist, D.C., Leavitt, B., Barrow, T., Holz, J.C., 2005. Assessing the potential of SeaWiFS and MODIS for estimating chlorophyll concentration in turbid productive waters using red and near-infrared bands. *Remote Sensing of environment*, 96, pp. 176-187.

Dekker, A.G., 1993. Detection of optical water parameters for eutrophic lakes by high resolution remote sensing. PhD. Dissertation, Free University, Amsterdam.

EPD, 2004. Marine water quality in Hong Kong in 2004, *Annual report provided by the Hong Kong Environmental Protection Department*, Hong Kong.

Gitelson, A., Garbuzov, G., Szilagyi, F., Mittenzwey, K-H., Karnieli, K., Kaiser, A., 1993. Quantitative remote sensing methods for real-time monitoring of inland waters quality. *International Journal of Remote Sensing*, 14(7), pp. 1269-1295.

Gons, HJ, 1999. Optical tele-detection of chlorophyll a in turbid inland waters. *Environmental Science & Technology*, 33, pp. 1127-1132.

Han, L.H., Jordan, K.J., 2005. Estimating and mapping chlorophyll-a concentration in Pensacola Bay, Florida using Landsat ETM+ data. *International Journal of Remote Sensing*, 26(23), pp. 5245-5254.

Han, Z., Jin, Y.Q., Yun, C.X., 2006. Suspended sediment concentrations in the Yangtze River estuary retrieved from the CMODIS data. *International Journal of Remote Sensing*, 27(19), pp. 4329–4336.

Hu, C.M., Chen, Z.Q., Clayton, T.D., Swarzenski, P., Brock, J.C., Muller-Karger, F.E., 2004. Assessment of estuarine water-quality indicators using MODIS medium-resolution bands: Initial results from Tampa Bay, FL. *Remote Sensing of Environment*, 93, pp. 423–441.

Justice, C.O., Townshend, J.R.G., Vermote, E.F., Masuoka, E., Wolfe, R.E., Saleous, N., Roy, D.P., Morisette, J.T., 2002. An overview of MODIS land data processing and product status. *Remote Sensing of Environment*, 83, pp. 3-15.

Koponen, S., Pulliainen, J., Kallio, K., Vepsäläinen, J., Hallikainen, M., 2001. Use of MODIS data for monitoring turbidity in Finnish Lakes. *The International Geoscience and Remote Sensing Symposium (IGARSS'01)*, Sydney, Australia, pp.3

Kneubühler, M., Gemperli, C., Schläpfer, D., Zah R., Itten, K., 2005. Determination of water quality parameters in Indian ponds using remote sensing methods, *Proceedings of 4th EARSeL Workshop on Imaging Spectroscopy*, Warsaw, pp. 301-315.

Li, S.H., Tang, J.W., Yun, C.X., 2002. A study on the quantitative remote sensing model for the sediment concentration in estuary. *Acta Oceanologica Sinica*, 24, pp. 51–58.

Miller, R.L., McKee, B.A., 2004. Using MODIS Terra 250m imagery to map concentrations of total suspended matter in coastal waters. *Remote Sensing of Environment*, 93, pp. 259-266.

Milton, J.S., Arnold, J.C., 1995. *Introduction to probability and statistics: Principles and applications for engineering and computing sciences*. McGraw-Hill Publishing Company, Singapore, pp. 811.

Mobley, C.D., 1994. *Light and water; Radiative transfer in natural waters*. Academic Press, Inc., San Diego, pp. 592.

Morton, B., Wu, S.S., 1975. The hydrology of the coastal waters of Hong Kong. *Environmental Research*, 10, pp. 319-347.

Tassan, S., 1987. Evaluation of the potential of the Thematic Mapper for Marine application. *International Journal of Remote Sensing*, 8, pp. 1455-1478.

Vermote, E.F., Tanre, D., Deize, J.L., Herman, M., Morcrette, J.J., 1997. Second simulation of the satellite signal in the solar spectrum, 6S: an overview. *IEEE Transaction on Geoscience and Remote Sensing*, 35, pp. 675-686.

Wong, M.S., Lee, K.H., Kim, Y.J., Li, Z.Q., Nichol, J.E., Emerson, N., 2007. Modeling of suspended solids and salinity in Hong Kong using Aqua/MODIS satellite images, *Korean Journal of Remote Sensing*, 23(3), pp. 1-9.

Woodruff D.L., Stumpf R.P., Scope J.A., Paerl H.W., 1999. Remote estimation of water clarity in optically complex estuarine waters. *Remote Sensing of Environment*, 68, pp. 41-52.

Wu, S. S., 1988. Marine pollution in Hong Kong: a review. *Asian Marine Biology*, 5, pp. 1-23.

Yeung, I.M.H., 1999. Multiple analysis of the Hong Kong Victoria Harbour water quality data. *Environmental Monitoring and Assessment*, 59, pp. 331-342.

ACKNOWLEDGEMENT

The authors wish to acknowledge the NASA Goddard Earth Science Distributed Active Archive Center for the MODIS Level IB and Level II images, the Hong Kong Environmental Protection Department for the marine data, and Mr Olympian Kwok for acquiring the data.

APPENDIX

Equations of models:

$$T1: T = L_{\text{MODIS-C1}}^2 * 162.827 + 3.940$$

$$T3: T = L_{\text{MODIS-C1}}^2 * 198.009 + 1.755$$

$$T6: T = L_{\text{MODIS-C1}}^{1.087} * 62.028 + 5.811$$

$$C2: \log(\text{Chl } a) = -3.453 + 2.503 * \left(\frac{\log(\text{MODIS}_i)}{\log(\text{MODIS}_k)} \right)$$

$$C4: \log(\text{Chl } a) = -1.668 + 1.431 * \left(\frac{\log(\text{MODIS}_i)}{\log(\text{MODIS}_k)} \right)$$

$$C6: \log(\text{Chl } a) = -0.910 + 0.887 * \left(\frac{\log(\text{MODIS}_i)}{\log(\text{MODIS}_k)} \right)$$

$$S2: \log(\text{SS}) = 0.319 + 1.789 * \frac{\text{MODIS}_i + \text{MODIS}_k}{\log(\text{MODIS}_j) / \log(\text{MODIS}_k)}$$

$$S4: \log(\text{SS}) = -0.213 + 4.018 * \frac{\text{MODIS}_i + \text{MODIS}_k}{\log(\text{MODIS}_j) / \log(\text{MODIS}_k)}$$

$$S6: \log(\text{SS}) = -0.426 + 8.002 * \frac{\text{MODIS}_i + \text{MODIS}_k}{\log(\text{MODIS}_j) / \log(\text{MODIS}_k)}$$